DOI: 10.2478/fas-2021-0006
FATIGUE OF AIRCRAFT STRUCTURES
Volume 2021: Issue 13, pp. 54-71

EXPERIMENTAL AND NUMERICAL STRESS STATE ASSESMENT IN REFILL FRICTION STIR SPOT WELDING JOINTS

Elżbieta Gadalińska[1] 0000-0002-8205-6539
Andrzej Kubit[2] 0000-0002-6179-5359
Tomasz Trzepieciński[2] 0000-0002-4366-0135
Grzegorz Moneta[1] 0000-0003-3899-1957
[1]Łukasiewicz Research Network – Institute of Aviation,
Al. Krakowska 110/114, 02-256 Warsaw, Poland
[2]Rzeszów University of Technology,
Al. Powstańców Warszawy 12, 35-959 Rzeszów, Poland

elzbieta.gadalinska@ilot.lukasiewicz.gov.pl

Abstract

Refill Friction Stir Spot Welding (RFSSW) is a technology used for joining solid materials that was developed in Germany in 2002 by GKSS-GmbH as a variant of the conventional friction stir spot welding (FSSW) [1]. In the RFSSW technology, the welding tool consists of a fixed outer part and rotating inner parts, which are called a pin and a sleeve. The tool for RFSSW is designed to plasticize the material of the parts to be joined by means of a rotary movement. The design of the tool allows independent vertical movement of both elements of the welding tool. This allows obtaining spot welds without creating holes that could weaken the structure. The main advantage of RFSSW is the potential for replacing the technologies that add weight to the structure or create discontinuities, such as joining with screws or rivets. Thus, RFSSW has great potential in the automotive, shipbuilding and aviation industries. Furthermore, the technology can be used to join different materials that could not be connected using other joining methods. The main objective of this work is to understand the physical and mechanical aspects of the RFSSW method – including the residual stress state inside the weld and around the joint. The results of the investigations can help to determine optimal parameters that could increase the strength and fatigue performance of the joint and to prove the significant advantage of RFSSW connections over other types of joints. The work assumes the correlation of two mutually complementary investigation methods: numerical analyses and experimental studies carried out with diffraction methods. The comparison between numerical and experimental results makes potentially possible the determination of degree of fatigue degradation of the material by observing the macroscopic stress state and the broadening of the diffraction peak width (FWHM), which is an indicator of the existence of micro-stress related to the dislocation density and grain size.

Keywords: RFSSW, X-ray diffraction, finite elements modelling, stress state, aluminium alloys
Article Category: Research Article

INTRODUCTION

Research carried out in the last decade has demonstrated that the RFSSW technology has great potential for joining aluminium alloys used in aircraft structures. The aim of most studies has been to determine the optimal welding parameters to achieve the maximum load of the joint while minimizing possible weld defects. As for now the RFSSW joints have been investigated with many different methods including both the experimental and numerical ones. Among the experimental methods, the following may be identified: SEM, acoustic microscopy, EBSD and X-ray diffraction. In this work, the X-ray diffraction was chosen as a prime methodology of the investigations. In Zhibo Dong's et al. [2], the RFSSW technology was used to connect sheets made of 5083 Al and AZ 31 alloys. The effect of rotation speed on joint formation, intermetallic components (IMCs) and failure load of the joint was studied. The results showed that differing between each other, Al/Mg alloys can be successfully connected using the RFSSW method. Moreover, the connections were obtained without defects. The diffraction methods were used there to determine the phase composition of the material inside the joint and thus allowed to show the intermetallic components inside the joint. Cao et al. [3] dealt with the evolution of the microstructure texture and mechanical properties during the RFSSW process for aluminium 6061-T6. The electron backscatter diffraction method was used to study the texture, and it showed the appearance of a significant shear texture. The study also examined the evolution of the microstructure in a RFSSW joint. Very extensive research was undertaken by Jambhale et al. [4], with regard to the flat friction stir spot welding for different aluminium sheets (two AA6082-T6 sheets and one AA6061-T6 sheet). Microstructural features of the joint such as microhardness and mechanical properties were examined in the context of such parameters as the tilt angle, tool rotational speed, dwell time and tool plunge depth. Other methods used were also optical microscopy, microhardness testing, lap shear strength test and X-ray diffraction measurements. Diffraction studies revealed the presence of compressive residual stresses due to forces exerted by the tool shoulder. Fractographic analyses were also performed. In this paper, the authors made a methodological error when calculating residual stresses. Stresses should be calculated based on diffraction peaks from high 2θ angles. Instead, the authors performed calculations for all possible diffraction peaks, which maximizes the calculation error to an unacceptable level. Lin et al. [5] undertook wide-ranging research on the microstructure, mechanical properties and stress corrosion behaviour for friction stir welded joints of Al-Mg-Si alloy extrusion. The evolution of the microstructure and the mechanical properties of RFSSW welds for 2A12-T4 alloy were studied by Li et al. [6]. The authors investigated the effects related to the tool speed value on the weld formation, microstructure evolution and mechanical properties. They suggested the existence of some characteristic macrostructure related to the way the plasticized material flows. The microstructure of the joint revealed changes in grain

size, the distribution of the precipitations, and the substructure in the direction parallel to the width. The authors noted the existence of a softened region, the formation of which may be associated with coarsening and dissolution of S-precipitations. Moreover, the cracks caused by the melting of S-precipitations were observed in the mixing zone of the joint. They were produced at the highest speed of welding. Wang et al. [7] conducted very interesting and extensive research on an innovative method of increasing the fatigue strength of welded joints made with the RFSSW method by using graphene nanosheets. The research methods used in the work included microstructure observation, crack characteristics, EBSD. Kubit [8] carried out high-cycle fatigue strength tests of single-lap welded joints. C-mode acoustic scanning microscopy (C-SAM) and scanning electron microscopy (SEM) were used to assess the joint quality and microstructure characteristics. The paper discusses the influence of maximum load force and defects related to material flow in the weld on the failure mechanism. Insufficient ductility of the sheet material and mixing of the material in the weld area were the key defects that affected the number of failure cycles. Defects in the welded joint construction were the source of a decrease in fatigue life compared to the fatigue life of defect-free joints. It was also found that defects in RFSSW welds can be effectively detected using the C-SAM non-destructive method. Kluz et al. [9] presented the analysis of the influence of tool immersion depth on shear strength. For this purpose, a shear load was applied to the specimens and shear strength was determined. The aim of Kubit et al. [10] work was an experimental study of fatigue damage in RFSSW. Samples for fatigue analysis were made of 7075-T6 aluminium alloy with a thickness of 0.8 mm and 1.6 mm, which are used in the production of aircraft fuselages consisting of a cladding coating with a stiffening string. The load capacity of the joints was determined by tensile/shear tests. Fatigue crack microstructure features for different levels of variable load were tested with Scanning Electron Microscopy. The analysis of fatigue cracks showed that the Alclad layer in the lower part of the weld is a kind of a structural notch and in this situation it can be the starting point of fatigue cracking. It was found that the crack mechanism depended on the load amplitude value. Analysis of SEM micrographs of fatigue cracks showed that the source of fatigue cracking was the thermal-mechanical influence zone and the heat influence zone.

The application of FEM in simulation studies related to friction welded joints can be divided into two categories: modelling the process of manufacturing a welded joint technological analysis [11, 12, 13, 14] and modelling of welded joints as structural elements (structural mechanics) [15, 16]. The first category includes simulation studies of the welding process in order to determine the course of the joint production process, taking into account friction phenomena, heat generation, bringing the material to a doughy state with mixing of components, as well as aspects of the change of material structure and physical state, and to determine the field of residual stresses and deformations in the joint area. The second category focuses on how the created connection works as an element of the loaded structure. The most common simulations in this area relate to the modelling of the behaviour of a point joint in statically or dynamically loaded structure. As part of the first above mentioned category there are plenty of works assuming different approaches. Yang et al. [17] used so called Smoothed Particle

Hydrodynamics (SPH) to approach the plunge stage in RFSSW aluminium. Material flow modes and material flow velocity were tested using an elastoplastic deformation model. This work contains only possible applications of SPH method in RFSSW simulation and no quantitative results or experimental validation were presented. Muci-Küchler et al. analyzed the plunge phase of RFSSW using the thermo-mechanical finite element method. The finite element model was developed in Abaqus/Explicit simulation enviroment. The predicted temperature distribution in the weld zone showed good compatibility with the experimental studies. The results of the material flow simulation during RFSSW for aluminium sheets 6161 were presented by Cao et al. [18]. The authors used the Abaqus program with Coupled Eulerial-Lagrangian (CEL) formulation, which takes into account the relationships between stress and temperature, strain and strain rate. The authors analyzed the influence of the process parameters ontheformation of the hook defect and onion structures near the sleeve periphery. FEM simulations designed to determine how process parameters affect the temperature distribution in the weld area were presented by D'Urso and Giardini [19]. The two-dimensional numerical model was validated experimentally showing a good ability to predict the shear resistance of the joint and the maximum temperature in the weld area. D'Urso et al. [20] conducted a numerical study on the distribution of temperature and weld force as a function of the welding parameters. A three-dimensional model using the finite element method was realized for AA6060 T6 aluminium sheets in the Deform program, assuming a rigid-plastic material model. Malik et al. [21] developed a three-dimensional model based on FE for FSSW using the commercial version of the Deform /Implicit code in order to select appropriate welding parameters for filling and exiting the weld hole. The FEM model related to the Arbitrary Lagrangian-Eulerian (ALE) method, based on Abaqus/Expicit software carried out by Yang et al. [22, p. 8], was capable of analysing the probeless FSSW process for aluminium alloy 2198-T8. The Johnson Cook equation was used to describe stress flow and its dependence on temperature, plastic deformation and strain rate. The fluid dynamic calculation technique is also widely used to simulate temperature distribution during the FSSW process. The 3D CFD model created in the ANSYS/Fluent code allows for the simulation of temperature control of the tool used during the friction welding process. In the model, the tool temperature was optimized to reduce the force in the axial direction applied by the tool. Atharifar et al. [23] used the CFD technique to simulate heat transfer and material flow during frictional welding of AA6061 aluminium alloy. Temperature-dependent material properties and stick / slip conditions were assumed in the numerical model. Recent developments and applications of CFD simulation for frictional welding analysis were presented by Chen et al. [24].

The calculations based on the SPH of RFSSW processes carried out by Yang et al. [17] apply only to the plunge stage. Furthermore, the correctness of the numerical models is difficult to verify because the only material parameters provided by the authors are the Poisson ratio and the Young modulus. The thermo-mechanical Muci-Küchler model [25] was also limited to the plunge stage. Kubit and Trzepieciński [26] used a two-dimensional axially symmetrical fully coupled thermo-mechanical model for RFSSW welds of Alclad 7075-T6 alloy in the form of aluminium sheets. The aim was to predict the material flow and temperature distribution in the weld area after all

the phases of the RFSSW process, i.e. touch, preheating, plunging, refilling and retreating. Temperature-dependent and strain rate material models of sheet metal and cladding layer were established. The results of numerical calculations were compared with the experimental results.

The main objective of the work presented here was to introduce the experimental basics in frames of the X-ray diffractometry for future investigation aimed to the understanding the physical and mechanical aspects of the RFSSW method. We suppose that it could help to determine the optimal parameters that could increase the strength of the joint and demonstrate the significant advantage of RFSSW connections over other types of joints used in aviation and the automotive industry. In our approach, we intended to correlate two mutually complementary investigation methods: numerical analyses and experimental results given mainly through diffraction methods.

While in the general analysis of large structures containing multiple welds such an approximation may give good results without significantly increasing the size of the problem, in the analysis of the local behaviour, as well as with regard to the welds themselves, such an approximation may be rather inaccurate. Therefore, there is a need to define an exact model of the welded joint for more accurate simulation studies with the Finite Element Method. This need is also emphasized in many publications on the problem of finding a better welding model [27]. In summary, modelling the work of welded joints requires the preparation of several weld models at different levels of generalization. A simple − for the calculation of large structures, where it is important to represent the weld with as few elements as possible, correctly determining both the strength and stiffness of the joint; a more sophisticated for local stress modelling of the most stressed nodes and very accurate for fatigue, dynamic calculations and diagnostic analyses. The objective in the frames of numerical modelling is the developing a calculation methodology to estimate the fatigue life of such connections.

On the other hand, as the experimental validation of numerical model is crucial. The development of diffraction methodologies for estimation the stress state, dislocation density and as a result the fatigue damage is necessary to validate the numerical calculations. Moreover, the data obtained from the experiments are the key parameters for numerical modelling of the phenomena during fatigue loading.

Despite the many advantages of the RFSSW technology over the traditional riveting, such as no need to drill a hole, no need to use a filler material, no porosity, no generated chipping, easy automation of the process, the RFSSW technology has not yet been fully understood. Appropriate selection of RFSSW parameters (process time, tool speed, tool cavity level) are crucial to ensure the adequate strength of the joint [28, 29]. The welding parameters are sensitive to many external factors such as the type of materials to be welded, the thickness of the sheets to be welded, material cladding, etc. Although many publications dealing with this issue are available, the guide to the optimal RFSSW process parameters for thin-walled aluminium structures are not still clearly defined. Summarizing, creation of RFSSW joints research methodology, which will allow to predict their static and fatigue properties and to model them at different levels of accuracy (generalization) in construction design is necessary.

RFSSW – THE METHOD DESCRIPTION.

Refill Friction Stir Spot Welding is a solid state joining technology with the potential to replace other types of joining in e.g. aerospace applications. The selection of proper parameters of this process is crucial in view of ensuring the mechanical strength of the joint. The main aim of this work was to experimentally investigate the residual stress state after fatigue tests with different characteristics and to perform the numerical calculations for the quasistatic tests of this type of joints. This technology can join dissimilar materials which are difficult to join using fusion welding due to different thermal expansion coefficients and melting points. A better understanding of the physical and mechanical aspects of the material flow could help to set optimal welding parameters which could improve the weld strength.

The welding tool used to prepare specimens for the diffraction experiment in the frame of this work was equipped with a welder and consists of three independent elements: a 17 mm diameter clamping ring, a 9 mm diameter sleeve and a 5.3 mm diameter pin. The RFSSW process can be briefly divided into four main stages: touchdown and preheating, plunging, refilling, and retreating. After the touchdown stage, the tool starts to rotate to preheat the material of the upper sheet (Fig. 1a). At the plunging stage, the rotating sleeve plunges into the metal, while the pin moves upwards (Fig. 1b). After reaching a certain plunge depth, the sleeve and pin reverse their direction and return to their original position (Fig. 1c). Finally, the tool is retracted from the workpiece (Fig. 1b).

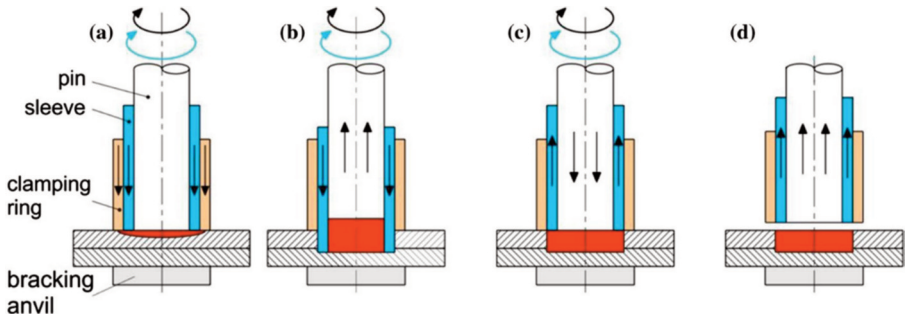

Fig. 1. Refill friction stir spot welding process [26].

MATERIAL AND SPECIMENS

The RFSSW joints for these investigations were made from 0.8 mm thick and 1.6 mm thick Alclad 7075-T6 aluminum alloy plates. This metal alloy is a kind of non-weldable lightweight material and is characterized by high mechanical strength, comparable to that of structural steel, and a very high fatigue resistance. It is a precipitation-hardened Al–Zn–Mg–(Cu) alloy that has been extensively used for highly loaded constructional elements in aircraft structural components. The sheets of this material were subjected to cladding, i.e. an aluminum alloy core of the material was covered with surface layers of pure aluminum. Specimens were prepared in an overlap joint, where the thicker sheet is set as the top one (Fig. 2). This configuration corresponds to the joining of a stringer (1.6 mm thick) to the skin (0.8 mm-thick) in aircraft structures.

The clamping force during the welding was 17 kN, tool rotational speed was 2600 rpm and the tool plunge depth was 1.5 mm. The welding cycle consisted of 1s three steps, i.e. plunge time (1 s), stirring time (1 s) and tool retract time (1 s).

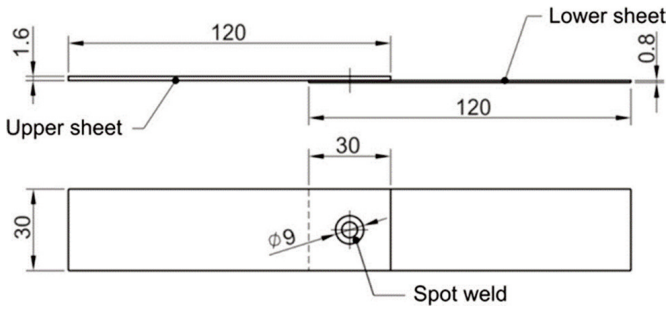

Fig. 2. The specimens subjected to the experiments.

For the X-ray experimental investigations there were prepared five types of specimens. Two of them were prepared for the analyses of the residual stresses for the investigation of the stress state for the initial state of the specimens, referred here as the *initial state*, directly after the welding process. For this case two different welding parameters were applied: Specimen I1 was welded with the spindle speed 2200 rpm, the tool plunge depth was 1.5 mm and the welding process lasted 2.5 s (Fig. 3). The tool plunge for the next specimen at the *initial state*, signed with I3 (Fig. 4) was the same but the spindle depth and welding time differed from the parameters for specimen I1: being respectively 2800 rpm and 1.5 s.

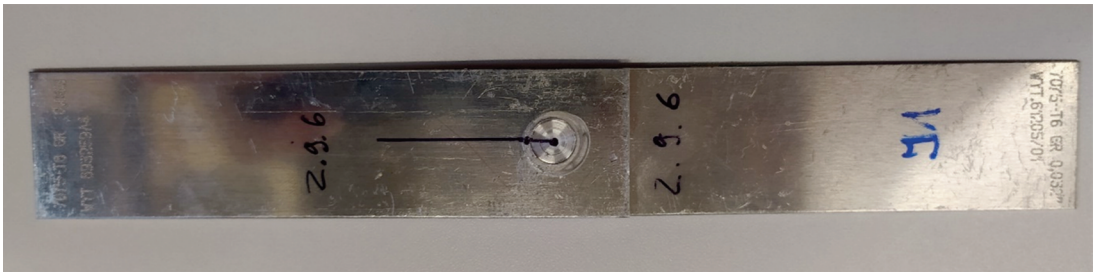

Fig. 3. Specimen I1 representing the *initial state* after the RFSSW process with following parameters: spindle speed – 2200 rpm, tool plunge depth – 1.5 mm, duration of welding – 2.5 s.

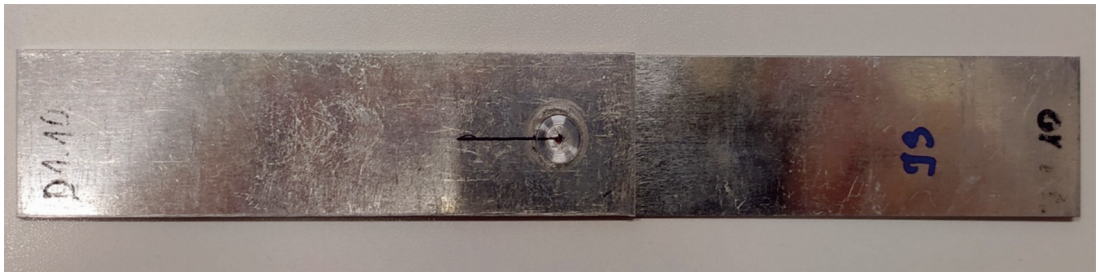

Fig. 4. Specimen I3 representing the *initial state* after the RFSSW process with following parameters: spindle speed – 2800 rpm, tool plunge depth – 1.5 mm, duration of welding − 1.5 s.

Another set of specimens was prepared to investigate the stress state around the welds after a number of fatigue cycles. These specimens (F1, F2 and F3) were welded with the same parameters as Specimen I1, with one exception: for Specimen F3 the tool plunge depth was bigger and equal to 1.8 mm. The specimens were subjected to fatigue tests, with high-cycle tests designed for two of them, F1 and F3, and for one: F2 − low cycle test. For Specimen F1, the maximum force was 0.9 kN and it was subjected to almost $25 \cdot 10^6$ fatigue cycles (Fig. 5). For Specimen F2, the maximum force was 2 kN at $17 \cdot 10^3$ cycles; for Specimen F3, the fatigue test parameters were $17 \cdot 10^3$ cycles and 1 kN, respectively.

Fig. 5. Specimen F1 after the fatigue tests: maximum force – 0.9 kN, $25 \cdot 10^6$ fatigue cycles.

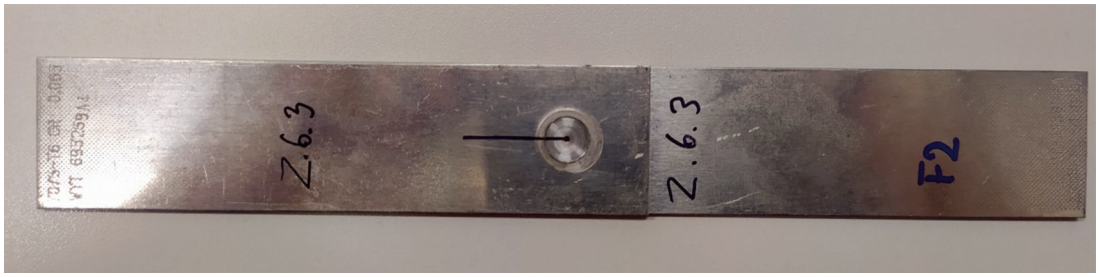

Fig. 6. Specimen F2 after the fatigue tests: maximum force – 2 kN, $17 \cdot 10^3$ fatigue cycles.

Fig. 7. Specimen F3 after the fatigue tests: maximum force – 1 kN, $17 \cdot 10^3$ fatigue cycles.

EXPERIMENT

Diffraction measurements

Measurements using X-ray diffraction methodology were carried out using a portable Xstress 3000 G2R diffractometer. The measurements were carried out for the surface layer of the samples and for the aluminum phase. The K alpha radiation of the chromium

X-ray tube was used and the measuring spot was 1 mm. The step between every measurement point was 1 mm too. The measurements were taken of the stress distribution along the centerline of the specimen starting from the focal point at the weld. Over a length of approx. 20 mm. The measurements were carried out for the circumferential and radial directions in relation to the geometry of the welds. All measurements were performed for the thicker, 1.6 mm sheet.

Phase aluminium	**E = 70.6 GPa** **ν = 0.345**	
measurement parameters	2θ/hkl	139.3° / 311
	exposure time	300 s
	measurement geometry	ψ
	φ	0°, 90°
	ψ (tils no. //range)	6 // −40° − +40°
	ψ oscillations	5°
	radiation	CrK_{α}
	collimator size	1 mm
calculation parameters	background subtraction	linear
	peak position	cross-correlation

Results

In the case of the specimen at the "initial" state I1, it can be observed that the stresses in the weld area are better defined by the applied measurement methodology – the errors are considerably lower than in the case of the native material of the welded sheets. Furthermore, it should be noted that in the weld the stresses in the circumferential direction are close to zero, whereas in the radial direction they are of 40 MPa and are of the compressive nature. In the parent material of the plate, the stress values are much more widely scattered and can be assumed to oscillate around zero for both directions.

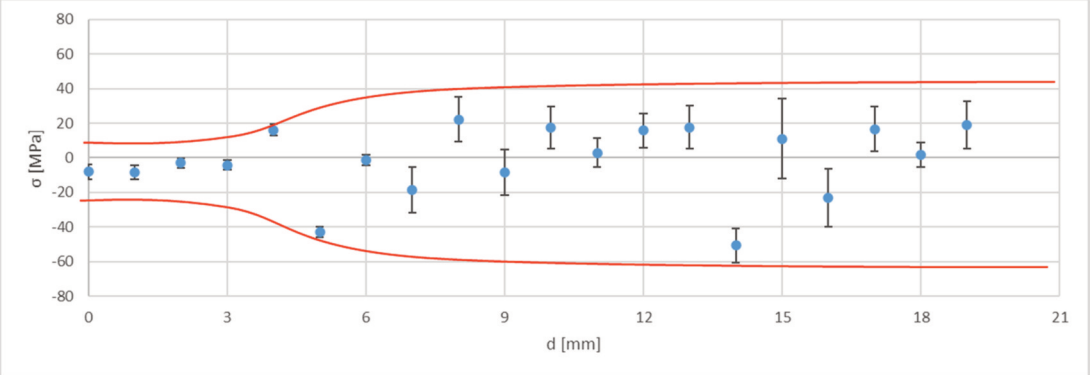

Fig. 8. Diffraction stress measurements for I1 specimen for tangential direction with respect to the weld geometry.

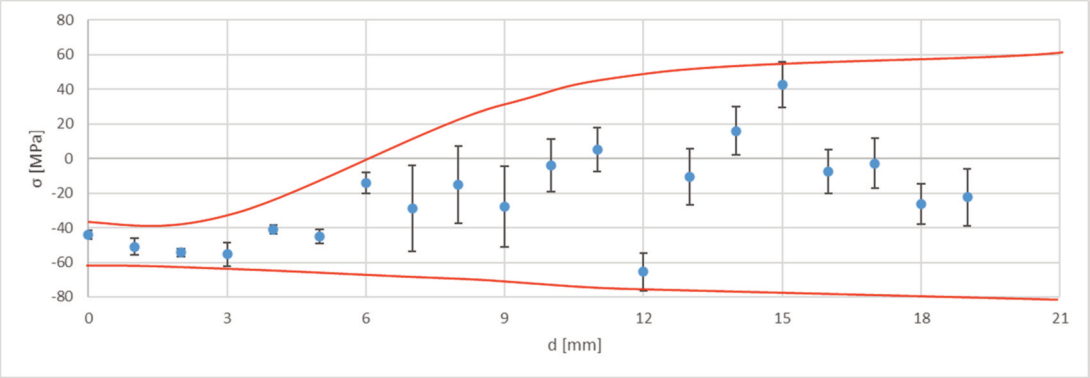

Fig. 9. Diffraction stress measurements for I1 specimen for radial direction with respect to the weld geometry.

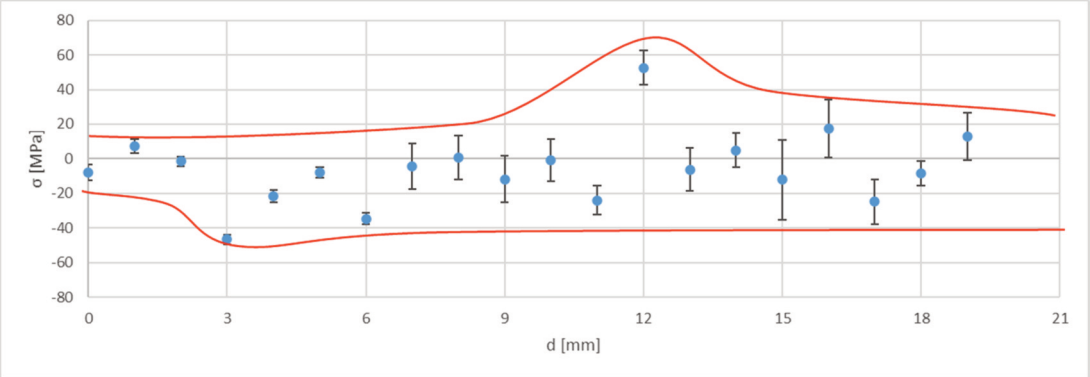

Fig. 10. Diffraction stress measurements for I3 specimen for tangential direction with respect to the weld geometry.

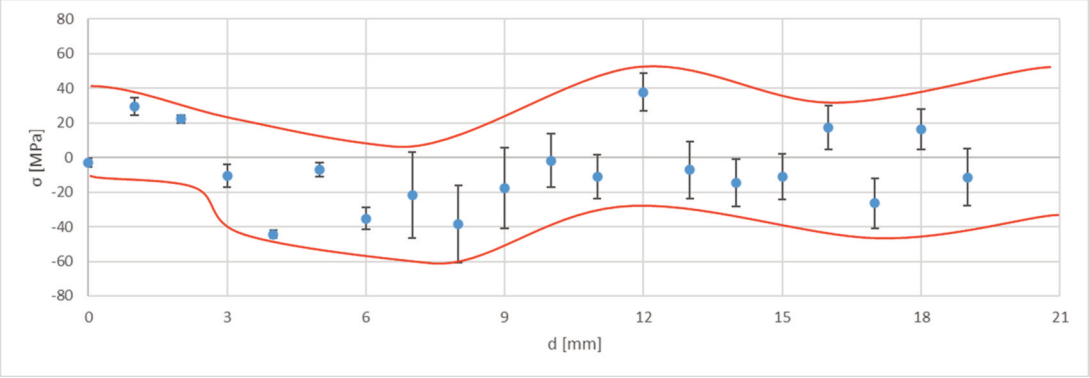

Fig. 11. Diffraction stress measurements for I1 specimen for radial direction with respect to the weld geometry.

If the welding parameters were changed, i.e., the number of rotations was increased at the expense of decreasing the duration of the process, as is the case of Specimen I3 there was no significant variation in the stress values for the directions for which the measurements were carried out (Figures 10 and 11). The stress values along the entire length of the examined section had the same value: they oscillated around zero.

It is worth mentioning that in the case of this sample, as in the case of sample I1, the values of measurement errors for the weld area were relatively small compared to the measurements obtained for the native material of the plates. This effect can be attributed to crystallographic texture release which can affect the accuracy of X-ray stress measurements.

The next two graphs concern stress measurements for specimens for which high-cycle fatigue tests were performed (F1 and F3, Figures 12−15). In the case of both specimens, there was no significant change in the stress level – for both of them, for both directions, the stress values oscillated around zero between approximately −40 and 40 MPa. It is worth noting that after realizing a higher number of fatigue cycles for Specimen F1, 25 millions of cycles, the measurement errors decreased too. It is likely that the high-cycle fatigue process affects the release of the crystallographic texture.

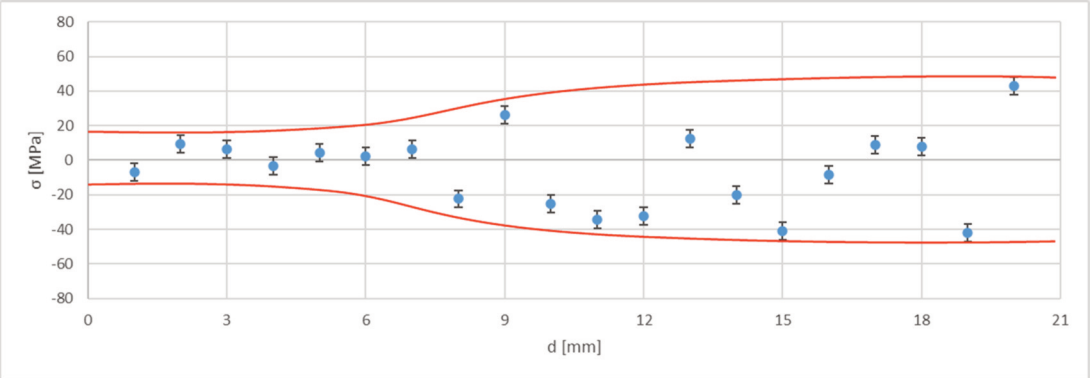

Fig. 12. Diffraction stress measurements for F1 specimen, after HCF testing, for tangential direction with respect to the weld geometry.

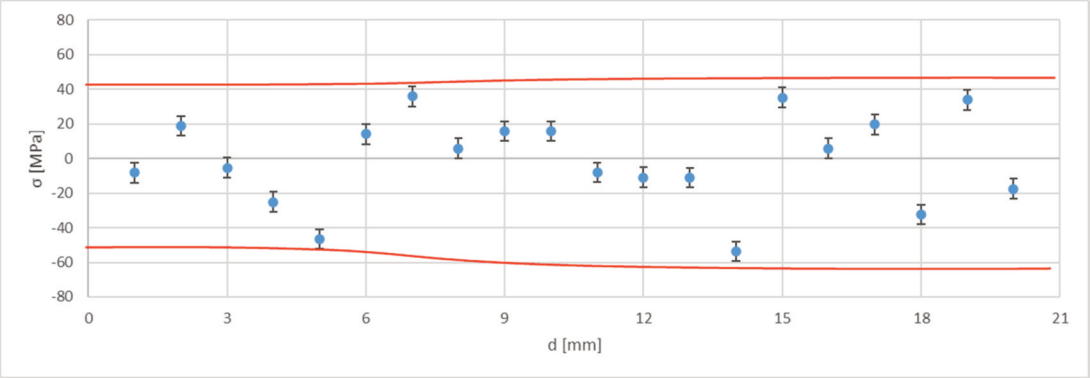

Fig. 13. Diffraction stress measurements for F1 specimen, after HCF testing, for radial direction with respect to the weld geometry.

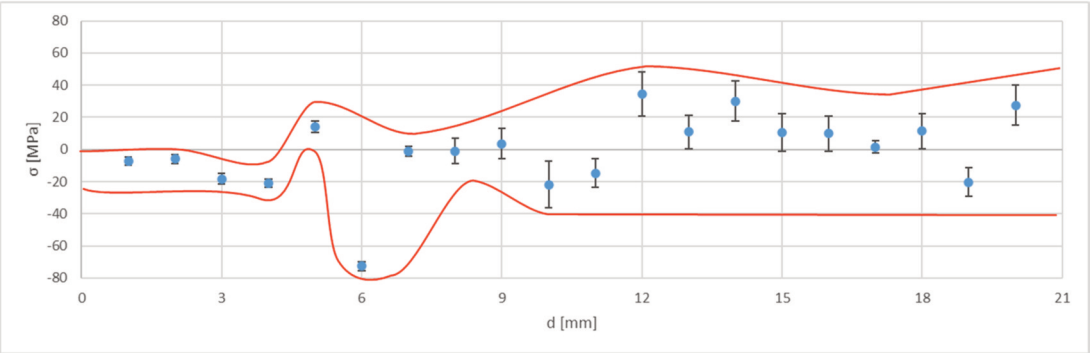

Fig. 14. Diffraction stress measurements for F3 specimen, after HCF testing, for tangential direction with respect to the weld geometry.

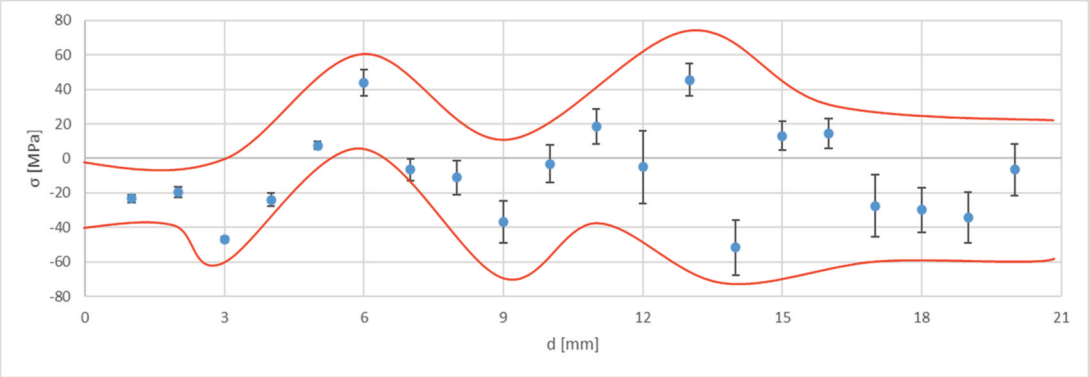

Fig. 15. Diffraction stress measurements for F3 specimen, after HCF testing, for radial direction with respect to the weld geometry.

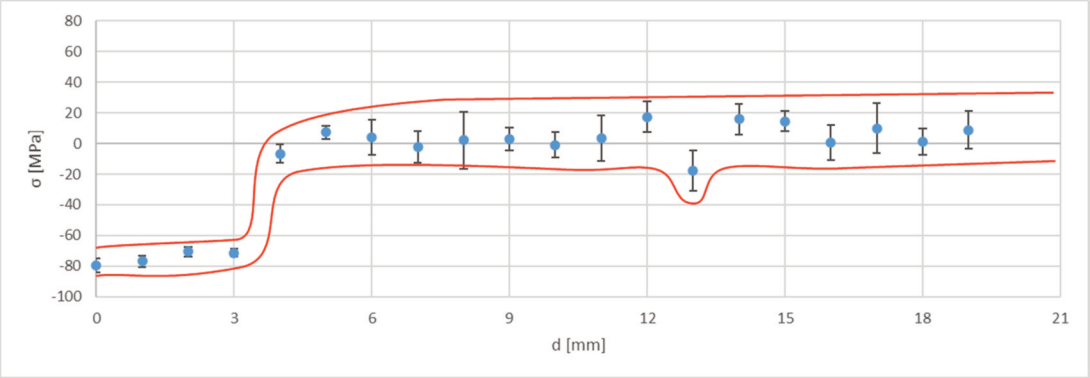

Fig. 16. Diffraction stress measurements for F2 specimen, after LCF testing, for tangential direction with respect to the weld geometry.

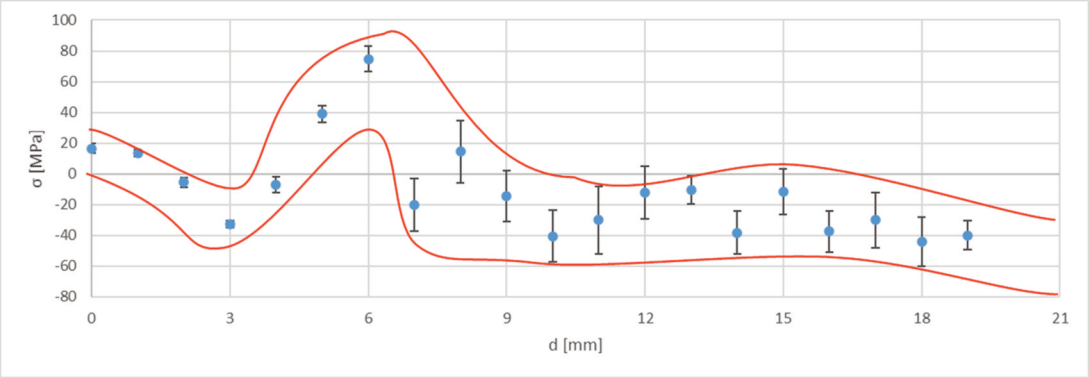

Fig. 17. Diffraction stress measurements for F2 specimen, after LCF testing, for radial direction with respect to the weld geometry.

Significantly different experimental results of stress measurements were obtained for the low-cycle fatigue specimen, Specimen F2 (Figures 16 and 17). Especially for the weld area, significantly different residual stress values for the circumferential direction could be seen in relation to the previously presented specimens as well as in relation to the stress values for the specimen's parent material. For the weld, these values oscillated around 80 MPa of compressive stresses while for the parent material they were around zero. A similar trend was not be observed for the radial direction, although in this case a change in the sign of the stresses in the parent material immediately behind the weld was seen. The stress values at this point were approx. 80 MPa of tensile stresses. It can be concluded that this may be the first sign of fatigue processes beginning.

Below, on Fig. 18, a comparison of the stress distributions in the welds and in the parent material of the plates for successive specimens subjected to different fatigue tests relative to the initial state Specimen I1, is presented. Differences in stress distributions between Specimen I1 and Specimens F1 and F3 (HCF) were not observable, whereas for the specimen subjected to LCF significant differences were visible.

Measurements of the half-width of the observed diffraction peaks were aimed at determining a degree of degradation of the crystalline structure of the weld material and the parent material due to fatigue processes. The presented graph shows that for fatigue-tested samples (red, blue and green lines), the values of half-widths were relatively lower than for the sample at the initial state. This observation may be an argument for the application of the method of measuring the half-width of diffraction peaks to determine the progress of fatigue processes by means of diffraction methods. This methodology still requires considerable refinement.

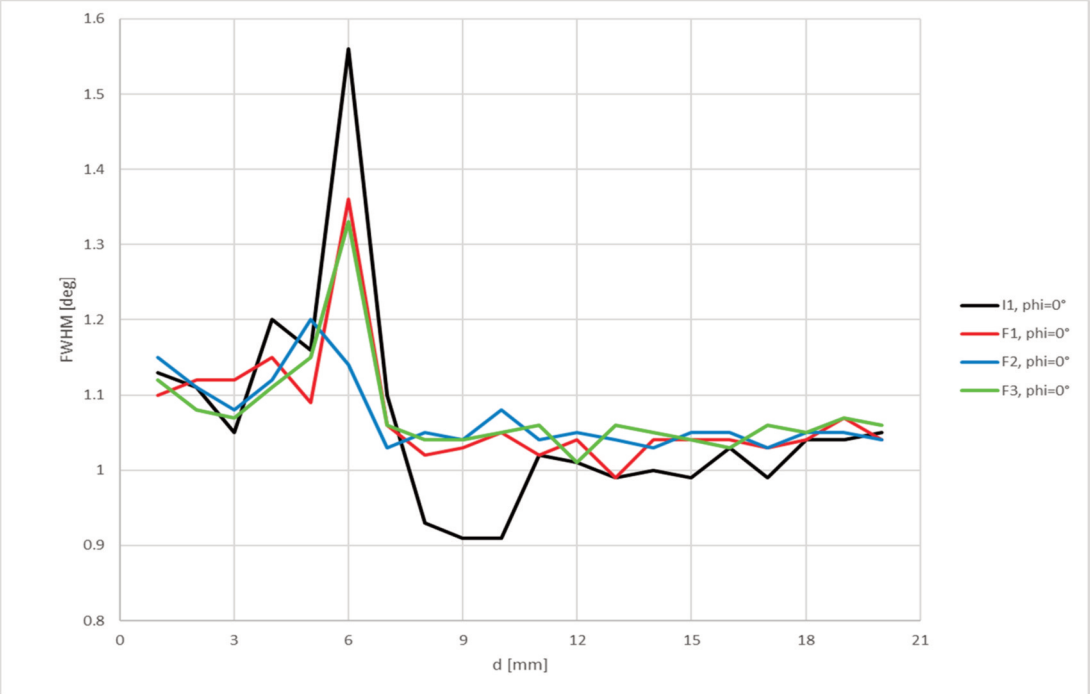

Fig. 18. The comparison of FWHM values for the specimen in the initial state (I1) and after the HCF (F1, F3) and LCF (F2) fatigue tests.

A preliminary Finite Element Analysis (FEA) was performed for the tensile test of the lap joint. The nonlinear simulation was performed in the ANSYS 2021R2 environment using SOLID185 elements (the geometry, mesh, load and boundary conditions are presented in (Fig. 19). In this preliminary study, the residual stress field from the RFSSW manufacturing process was not considered.

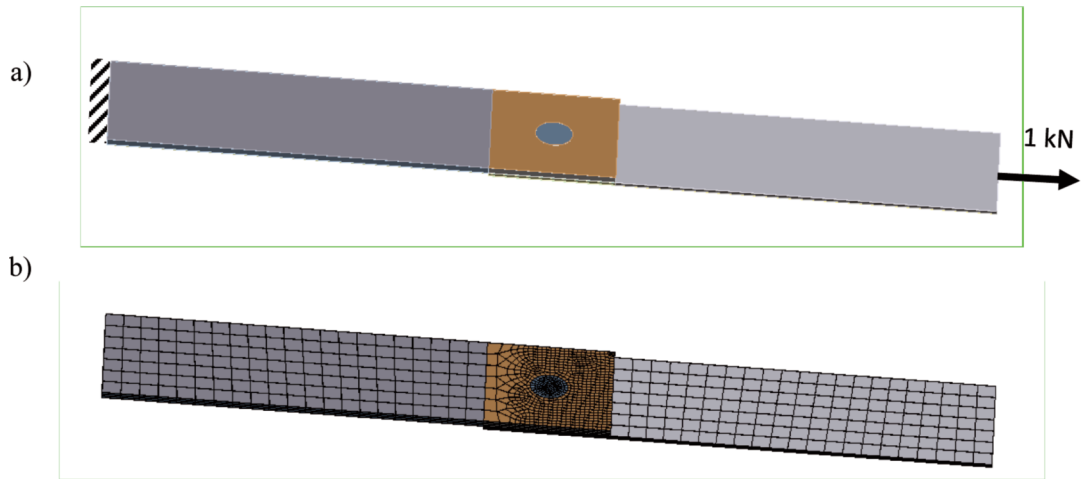

Fig. 19. Geometry of the lap joint with load and boundary conditions (a) and FEM mesh (b).

The FEA results of this study are presented in Fig. 20. The applied force of 1 kN caused significant secondary bending of the lap joint due to non-symmetrical nature of this joint type. Furthermore, it can be observed that the highest reduced stress peak (Huber-Mises-Hencky formulation, H-M-H) is located between the welded sheets near the weld joint, which corresponds to the recognized damage mechanisms (example presented in Fig. 21). More detailed FEM assessments requires considering residual stress distributions obtained from X-ray diffraction measurements and are planned for future studies. Based on them, the damage mechanism of RFSSW joints will be described and understood much better, which will be helpful to improve and optimize this technology for aviation structures.

Fig. 20. FEA results of the lap joint loaded by 1 kN
(H-M-H reduced stress field, deformation scaled 20 times).

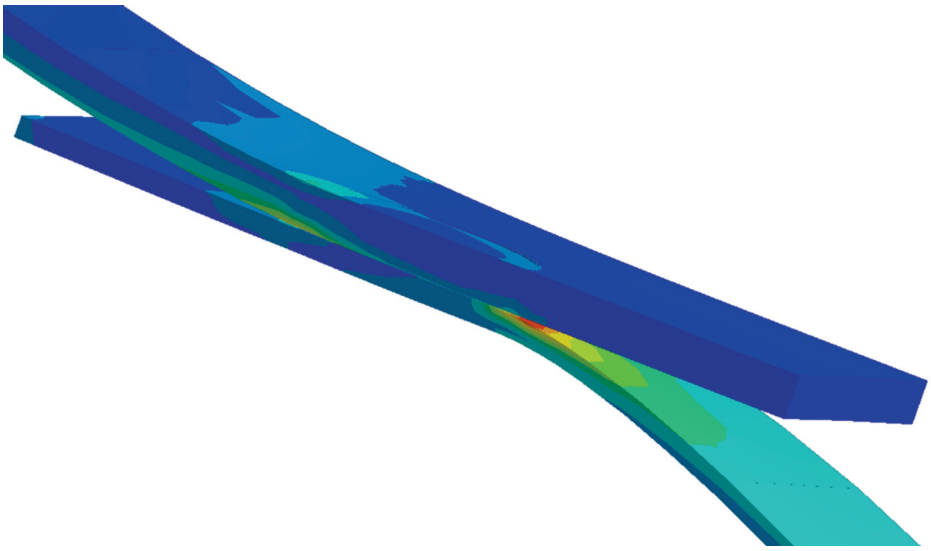

Fig. 21. One of recognized damage mechanisms of the RFSSW lap joint.

CONCLUSIONS

Preliminary stress measurements along the axes of the welded specimens showed the possibility of obtaining reliable information on the stress distribution after a certain number of fatigue test cycles. When testing a welded specimen subjected to low-cycle fatigue, significant changes in the stress distribution were observed in the weld area starting from the weld centre point. The measurements of the half-widths of diffraction peaks should, after further development of the methodology, allow researchers to determine the extent of fatigue processes in the weld and in the parent material of welded sheets. The preliminary FEA studies performed show good correlation of the peak stress location with the damage mechanisms observed. Considering the residual stress field in numerical simulations (which is planned for next studies) will contribute to a better understanding of damage phenomena that occurr in RFSSW joints and will help in more accurate fatigue assessment and optimization of this joining technology for aviation structures.

REFERENCES

[1] Schilling, C. and dos Santos, J. (2004). "Method and device for joining at least two adjoining work pieces by friction welding," US6722556B2, Apr. 20, 2004 Accessed: Nov. 28, 2020. [Online]. Available: https://patents.google.com/patent/US6722556B2/en.

[2] Dong, Z., Hu, W., Ai, X. and Lv, Z. (2019). Effect of Rotation Speed on Intermetallic Compounds and Failure Load of RFSSW-ed Dissimilar Al/Mg. *Trans Indian Inst Met*, 72(9), 2249–2256, doi: 10.1007/s12666-019-01672-6.

[3] Cao, J.Y., Wang, M., Kong, L., Zhao, H.X. and Chai, P. (2017). Microstructure, texture and mechanical properties during refill friction stir spot welding of 6061-T6 alloy. *Materials Characterization*, 128, 54–62, doi: 10.1016/j.matchar.2017.03.023.

[4] Jambhale, S., Kumar, S. and Kumar, S. (2020). A Novel Flat Friction Stir Spot Welding of Triple Sheet Dissimilar Aluminium Alloys: Analyzing Mechanical Properties and Residual Stresses at Weld Region. *Trans Indian Inst Met*, 73(9), 2205–2220, doi: 10.1007/s12666-020-02025-4.

[5] Lin, S., Deng, Y.L., Lin, H.Q. et al. (2018). Microstructure, mechanical properties and stress corrosion behavior of friction stir welded joint of Al–Mg–Si alloy extrusion. *Rare Met*., doi: 10.1007/s12598-018-1126-7.

[6] Li, G., Zhou, L., Luo, L., Wu, X. and Guo, N. (2019). Microstructural evolution and mechanical properties of refill friction stir spot welded alclad 2A12-T4 aluminum alloy. *Journal of Materials Research and Technology*, 8(5), 4115–4129, doi: 10.1016/j.jmrt.2019.07.021.

[7] Wang, S. et al., (2020). Strengthening and toughening mechanisms in refilled friction stir spot welding of AA2014 aluminum alloy reinforced by graphene nanosheets. *Materials & Design*, 186, 108212, doi: 10.1016/j.matdes.2019.108212.

[8] Kubit, A., Trzepiecinski, T., Faes, K., Drabczyk, M., Bochnowski, W. and Korzeniowski, M. (2019). Analysis of the effect of structural defects on the fatigue strength of RFSSW joints using C-scan scanning acoustic microscopy and SEM. *Fatigue & Fracture of Engineering Materials & Structures*, 42(6), 1308–1321, doi: 10.1111/ffe.12984.

[9] Kluz, R., Kubit, A. and Wydrzyński, D. (2018). The Effect of Plunge Depth on the Strength Properties of Friction Welded Joints Using the RFSSW Method. *Adv. Sci. Technol. Res. J.*, 12(1), 41–47, doi: 10.12913/22998624/76547.
[10] Kubit, A., Trzepiecinski, T., Bochnowski, W., Drabczyk, M. and Faes, K. (2019). Analysis of the mechanism of fatigue failure of the Refill Friction Stir Spot Welded overlap joints. *Archives of Civil and Mechanical Engineering*, 19(4), 1419–1430, doi: 10.1016/j.acme.2019.09.004.
[11] Jedrasiak, P. and Shercliff, H.R. (2019). Small strain finite element modelling of friction stir spot welding of Al and Mg alloys. *Journal of Materials Processing Technology*, 263, 207–222, doi: 10.1016/j.jmatprotec.2018.07.031.
[12] Meyghani, B. ,Awang, M.B., Emamian, S.S., Mohd Nor, M.K.B. and Pedapati, S.R. (2017). A Comparison of Different Finite Element Methods in the Thermal Analysis of Friction Stir Welding (FSW). *Metals*, 7(10), 450, doi: 10.3390/met7100450.
[13] Meyghani, B., Awang, M. and Wu, C.S. (2020). Finite element modeling of friction stir welding (FSW) on a complex curved plate. *Journal of Advanced Joining Processes*, 1, 100007, doi: 10.1016/j.jajp.2020.100007.
[14] Yu, M., Li, W.Y., Li, J.L. and Chao, Y.J. (2012). Modelling of entire friction stir welding process by explicit finite element method. *Materials Science and Technology*, 28(7), 812–817, doi: 10.1179/1743284711Y.0000000087.
[15] He, X., Gu, F. and Ball, A. (2014). A review of numerical analysis of friction stir welding. *Progress in Materials Science*, 65, 1–66, doi: 10.1016/j.pmatsci.2014.03.003.
[16] Yunus, M. and Alsoufi, M.S. (2018). Mathematical Modelling of a Friction Stir Welding Process to Predict the Joint Strength of Two Dissimilar Aluminium Alloys Using Experimental Data and Genetic Programming. *Modelling and Simulation in Engineering*, 2018. https://www.hindawi.com/journals/mse/2018/4183816/ (accessed Nov. 30, 2020).
[17] Yang, H., Yang, H. and Hu, X. (2015).Simulation on the plunge stage in refill friction stir spot welding of Aluminum Alloys. In Proceedings of the 4th International Conference on Mechatronics, Materials, Chemistry and Computer Engineering 2015. doi: 10.2991/icmmcce-15.2015.105.
[18] Cao, J.Y., Wang, M., Kong, L., Yin, Y.H. and Guo, L.J. (2017). Numerical modeling and experimental investigation of material flow in friction spot welding of Al 6061-T6. *Int J Adv Manuf Technol*, 89(5), 2129–2139, doi: 10.1007/s00170-016-9247-3.
[19] D'Urso, G. and Giardini, C. (2016). Thermo-Mechanical Characterization of Friction Stir Spot Welded AA7050 Sheets by Means of Experimental and FEM Analyses. *Materials*, 9(8), 689, doi: 10.3390/ma9080689.
[20] D'Urso, G. (2015). Thermo-mechanical characterization of friction stir spot welded AA6060 sheets: Experimental and FEM analysis. *Journal of Manufacturing Processes*, 17, 108–119, doi: 10.1016/j.jmapro.2014.08.004.
[21] Malik, V., Sanjeev, N.K., Hebbar, H.S. and Kailas, S.V. (2014). Finite Element Simulation of Exit Hole Filling for Friction Stir Spot Welding – A Modified Technique to Apply Practically. *Procedia Engineering*, 97, 1265–1273, doi: 10.1016/j.proeng.2014.12.405.
[22] Yang, X. et al. (2018). Numerical modelling and experimental investigation of thermal and material flow in probeless friction stir spot welding process of Al 2198-T8. *Science and Technology of Welding and Joining*, 23(8), 704–714, doi: 10.1080/13621718.2018.1469832.

[23] Atharifar, H., Lin, D. and Kovacevic, R. (2009). Numerical and Experimental Investigations on the Loads Carried by the Tool During Friction Stir Welding. *J. of Materi Eng and Perform*, 18(4), 339–350, doi: 10.1007/s11665-008-9298-1.

[24] Chen, G., Shi, Q. and Zhang, S. (2018). Recent Development and Applications of CFD Simulation for Friction Stir Welding. In Laurentiu Nastac, Koulis Pericleous, Adrian S. Sabau, Lifeng Zhang, Brian G. Thomas (Eds.) *CFD Modeling and Simulation in Materials Processing 2018*, (113–118), Springer, doi: 10.1007/978-3-319-72059-3_11.

[25] Muci-Küchler, K.H., Kalagara, S. and Arbegast, W.J. (2010). Simulation of a Refill Friction Stir Spot Welding Process Using a Fully Coupled Thermo-Mechanical FEM Model. *J. Manuf. Sci. Eng*, 132(1), doi: 10.1115/1.4000881.

[26] Kubit, A. and Trzepiecinski, T. (2020). A fully coupled thermo-mechanical numerical modelling of the refill friction stir spot welding process in Alclad 7075-T6 aluminium alloy sheets. *Archiv. Civ. Mech. Eng*, 20(4), 117, doi: 10.1007/s43452-020-00127-w.

[27] Borino, G., Fratini, L. and Parrinello, F. (2009). Mode I failure modeling of friction stir welding joints. *Int J Adv Manuf Technol*, 41(5), 498–503, doi: 10.1007/s00170-008-1498-1.

[28] Venukumar, S. Yalagi, S. and Muthukumaran, S. (2013). Comparison of microstructure and mechanical properties of conventional and refilled friction stir spot welds in AA 6061-T6 using filler plate. *Transactions of Nonferrous Metals Society of China*, 23(10), 2833–2842, doi: 10.1016/S1003-6326(13)62804-6.

[29] Rosendo, T. et al. (2011). Mechanical and microstructural investigation of friction spot welded AA6181-T4 aluminium alloy. *Materials & Design*, 32(3), 1094–1100, doi: 10.1016/j.matdes.2010.11.017.